Int. J. Heat Mass Transfer. Vol. 11, pp. 1657–1673. Pergamon Press 1968. Printed in Great Britain

TURBULENT HEAT TRANSFER FROM SMOOTH AND ROUGH SURFACES

R. A. GOWEN† and J. W. SMITH‡

Department of Chemical Engineering and Applied Chemistry, University of Toronto, Toronto, Canada

(*Received* 31 *July* 1967 *and in revised form* 4 *April* 1968)

Abstract—Radial temperature profiles have been obtained in a 2-in I.D. rough tube of equivalent sand roughness equal to 0·05 for Prandtl numbers of 0·7, 5·9 and 14·3 over a Reynolds number range 10000–50000. Plots of t^+ against log y/R are linear as in the case of u^+ for rough and smooth tubes, but the slope depends on Prandtl number and inferentially on the roughness. The t^+ intercept at log $y/R = 0$ is strongly dependent on the Reynolds number, unlike u^+ in turbulent rough pipe flow. An expression for the relation between t^+ and log y/R is presented, but the dependence of the slope A_R on roughness remains to be determined. The heat-transfer efficiency St/C_F was less in rough tubes than smooth ones for all the fluids studied, but the relative difference becomes smaller at higher Prandtl number and in the turbulent transition region. Friction factors and heat-transfer coefficients have also been measured in seven different $\frac{1}{2}$-in I.D. rough pipes of known surface geometry. Equivalent sand roughnesses ranged from 0·021 to ·095 for the pipes studied. A semi-theoretical equation based on the temperature profiles obtained in the 2-in pipe predicts the results of the present study and Nunner's air results adequately. It underestimates the water results of Dipprey.

NOMENCLATURE

A,	constant in the dimensionless velocity and temperature laws;
B,	constant in the dimensionless velocity and temperature laws;
C_F,	Fanning friction factor;
C_{FS},	Fanning friction factor for a smooth pipe;
C_p,	specific heat [Btu/lb °F];
D,	diameter [ft];
e,	roughness height [ft];
e_s, e_s/D,	the equivalent sand roughness;
f,	denotes a function;
g,	function in rough surface velocity profiles;
g_c,	gravitational constant;
h,	heat-transfer coefficient [Btu/h ft^2 °F];
L,	length of exchanger section [ft];
ΔP,	pressure drop [lbf/ft^2];
$\dot{q}$,	heat flux [Btu/h ft^2];
R,	pipe radius [ft];
t,	temperature [°F];
u,	point average velocity [ft/h];
u^*,	friction velocity, $\sqrt{(\tau_w g_c/\rho)}$ [ft/h];
w,	mass flow rate [lb/h];
y,	distance from wall [ft].

Dimensionless groups

Pr,	Prandtl number, $C_p\mu/k$;
Pr_t,	turbulent Prandtl number, ϵ_M/ϵ_H;
$\mathcal{R}$,	dimensionless radial position, r/R;
Re,	Reynolds number, Du_B/ν;
Re^*,	shear Reynolds number, Du^*/ν;
St,	Stanton number, $h/u_B\rho C_p$;
t^+,	dimensionless temperature, $(t_w - t)\rho u^* C_p/\dot{q}_w$;
u^+,	dimensionless velocity, u/u^*;
U,	dimensionless velocity, $u/u_{℄}$;
y^+,	dimensionless distance, yu^*/ν;
y/R,	dimensionless distance.

Greek symbols

α,	thermal diffusivity, $k/\rho C_p$ [ft^2/h];
ϵ_H,	thermal eddy diffusivity [ft^2/h];

† R. Shriver Associates, Denville, New Jersey, U.S.A.

‡ University of Toronto.

ϵ_M, momentum eddy diffusivity [ft^2/h];
μ, molecular viscosity [lb/ft h];
ν, kinematic viscosity [ft^2/h];
ρ, density [lb/ft^3];
ψ, function in the rough surface temperature profile;
ε, function in rough surface velocity profile.

Subscripts
B, bulk;
℄, centre line;
H, pertaining to heat transfer;
M, pertaining to momentum transfer;
R, pertaining to a rough surface;
w, pertaining to the wall.

TEMPERATURE PROFILES IN A ROUGH PIPE

Most studies of heat transfer in rough pipes have consisted of experimental measurements of heat-transfer coefficients and friction factors. Only a very few measurements of temperature profiles in rough pipes by which theoretical models can be tested have been made.

Many theoretical and experimental studies have been based on the analogy between heat and momentum transfer over smooth surfaces but unfortunately, the theoretical proposals have often out-distanced the experimental results. However, in recent experimental studies by the authors [1, 8] it was shown that dimensionless temperature and velocity profiles are similar over a Prandtl number range from 0·026 to 14·3 for turbulent flow in a smooth tube. The temperature profiles were presented in the form:

$$t^+ = A \ln y^+ + B \tag{1}$$

where A, to a slight extent, and B are functions of the Prandtl number only.

Rough surface heat and momentum transfer

The most complete study of velocity profiles over rough surfaces was done by Nikuradse [2]. Nikuradse glued sized sand particles inside tube walls and measured velocity profiles and pressure losses in water for a wide range of flow conditions. In his analysis Nikuradse showed that there was a unique relationship between the pressure losses and the velocity profiles and,

$$u^+ - 2{\cdot}5 \ln y/e = g[eu^*/\nu] \tag{2}$$

$$\sqrt{(2/C_F)} - 2{\cdot}5 \ln R/e + 3{\cdot}75 = g[eu^*/\nu]. \tag{3}$$

In the fully rough regime the function $g[eu^*/\nu]$ became constant and equal to 8·48. This occurred for values of eu^*/ν greater than fifty-five.

Moore [3] and later Clauser [4] used Nikuradse's data to show that away from the immediate vicinity of the wall the velocity profile for turbulent flow in a rough pipe could be described in terms of the smooth tube velocity distribution plus a simple shift in u^+. Thus,

$$u^+ = 2{\cdot}5 \ln y^+ + 5{\cdot}5 - \frac{\Delta u}{u^*}. \tag{4}$$

The function $\Delta u/u^*$ depends on the type and magnitude of the roughness and it increases with increasing roughness.

These studies suggest the value of obtaining temperature profiles in turbulent rough pipe flow for comparison with rough surface velocity profiles. This paper presents part of the results of a systematic study done at the University of Toronto for a doctoral thesis [5] on temperature profiles for turbulent heat transfer from a rough pipe. Data on temperature profiles and heat-transfer coefficients have been obtained for air ($Pr = 0{\cdot}7$), water ($Pr = 5{\cdot}7$) and 30% aqueous ethylene glycol ($Pr = 14{\cdot}3$) for a Reynolds number range from 10000 to 50000.

Experimental. A centrifugal pump was used to pump the water and the aqueous ethylene glycol solutions through the test section which formed a closed loop with a 45-gal storage drum. One of two calibrated rotameters was used to measure the flow rate. The temperature of the fluid was controlled by routing part of the stream through a cold water shell-and-tube heat exchanger where heat added in the test section and by the pump was removed. Fluid temperatures at the test section inlet and outlet were measured with thermocouples. The centrifugal pump and storage drum were disconnected from the flow system when air was being used as the test fluid. Air entered the system on the discharge side of the pump and flowed through the same exchanger, rotameters and test section as previously stated. Air was supplied by a large positive displacement blower connected to two large surge tanks.

The heat-transfer test section consisted of a smooth 2-in brass pipe, 24-in long. The wall was roughened by tinning and then soldering a 12 mesh brass screen to the inside surface of the pipe. The wall temperatures were measured by twelve, 32-gauge copper–constantan thermocouples attached to the tube wall and spaced at intervals along the heating section of the test pipe. The heating section was made by concentrically placing the brass pipe in a 2·625-in O.D. copper tube and pouring molten solder in the annulus. The outside surface was then covered with a thin layer of Teflon film and then uniformly wrapped with a ribbon resistance heater, see Fig. 1. The diameter of the rough tube was assumed to be that of an equi-volumed cylinder of the same length.

Current to the resistance heater was supplied and regulated by a variable auto-transformer connected to a 110 V a.c. outlet. The heat input was calculated from the wattage as measured by an appropriate a.c. wattmeter. The electrical power input and the sensible heat gain of the fluid as calculated by $wC_p(t_{B_{out}} - t_{B_{in}})$ agreed to within ± 5 per cent.

Radial temperature profiles were measured by a travelling thermocouple which traversed the radius of the pipe in a plane 2·0 in below the top of the heating element. A 32 gauge copper–constantan thermocouple, encased in a 0·0625-in O.D. stainless steel tube, was passed through a packed fitting in the pipe wall, and bent 90° downward to point into the flow. The tube containing the thermocouple was fixed to a sliding carriage whose radial position was controlled to within 0·001 in by means of a micrometer spindle. The thermocouple was flattened slightly to a thickness of 0·008 in, and fixed into the end of the tube with epoxy resin (Fig. 2).

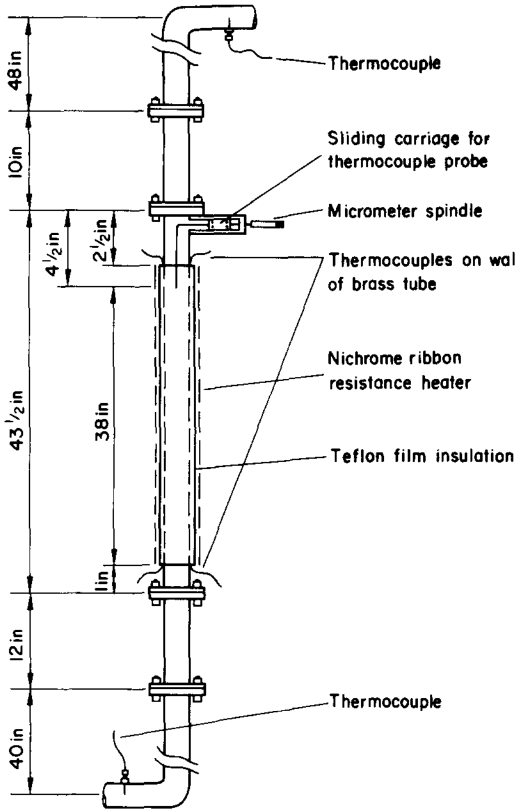

FIG. 1. Diagram of the heat-transfer section.

The thermocouples were connected to a Microcord mV recorder by a two pole, multi-contact switch. The wall temperatures were measured using the thermocouple in the test section inlet as a reference junction. An ice junction was used for standardization and for reading stream temperatures.

In all runs, temperature profiles were measured to within 0·005 in of the wall with a probable accuracy of $\pm 0{\cdot}001$ in and $\pm 0{\cdot}1$ degF. Pipe wall temperatures were also accurate to $\pm 0{\cdot}15$ degF. Pressure losses were measured with a simple carbon tetrachloride manometer with tap stations 22 in apart.

The friction factor was calculated from the measured pressure differentials and fluid properties for each run using the equation

$$C_F = \frac{\Delta P\, D\, g_c}{2\rho U_B^2 L}.$$

Fluid properties and Prandtl number were evaluated at the film temperature, $t_f = (t_w + t_b)/2$. The bulk temperature was maintained at about 75°F, and the temperature differences $t_w - t_b$ are tabulated in degF for the runs in Table 3.

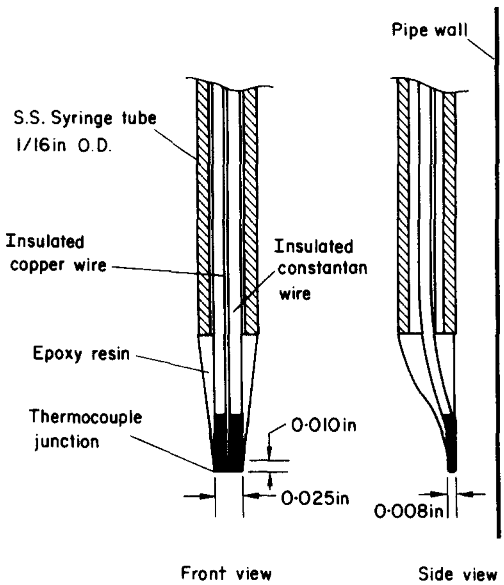

FIG. 2. Detailed diagram of the tip of the traversing thermocouple.

Experimental considerations limited the rough entry length to nineteen pipe diameters. Although the requirement for a developed velocity profile is about 40–50 l/D in smooth tubes, Logan and Jones [6] showed that in rough tubes, transition from a developed smooth to developed rough profile required only 8–10 diameters. Sleicher and Tribus [7] reviewed studies of seven investigators and concluded that 5–10 diameters are required for development of constant heat-transfer coefficients. The temperature profiles obtained in this study are of constant semi-logarithmic slope from the wall region to almost the centre of the pipe, suggesting that nineteen l/D's are sufficient for rough pipe temperature profiles.

Discussion of results†

The friction factor for the rough test section $R - 1$ is shown in Fig. 14 as log C_F vs. log Re

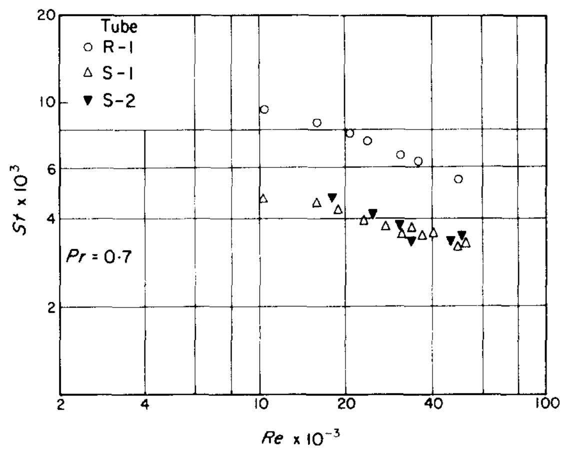

FIG. 3. Stanton number as a function of Reynolds number in test sections S-1, S-2 and R-1 with water.

as well as a line representing the smooth tube friction factor and given by:

$$C_F = 0{\cdot}046/Re^{0{\cdot}2}. \tag{5}$$

The equivalent sand roughness was calculated from the fully rough friction factor using equation (3). For the screen-type roughness used in the present study the equivalent sand roughness is approximately twice the measured roughness ratio as shown in Table 1. Similar large differences between e/D and e_s/D were observed by Nikuradse [2] for rib type roughnesses.

Heat-transfer coefficients for the rough surface test section are compared with the smooth tube values of [1] in Figs. 3–5. Most studies in the past have shown that for fully turbulent flow with fluids of a moderate Prandtl number the

† A complete set of numerical data for both Parts are available from the Documentation Centre for Unpublished Data, National Research Council, Ottawa 2, Canada.

increase in the friction factor is greater than the relative increase in the heat-transfer coefficient. This result has been verified in the present study and is illustrated in Fig. 6 where St/C_F is plotted against Re on logarithmic coordinates for smooth and rough surfaces. This figure also

Table 1

Measured e/D	Calculated e_s/D sand roughness [equation (3)]
0·027	0·051

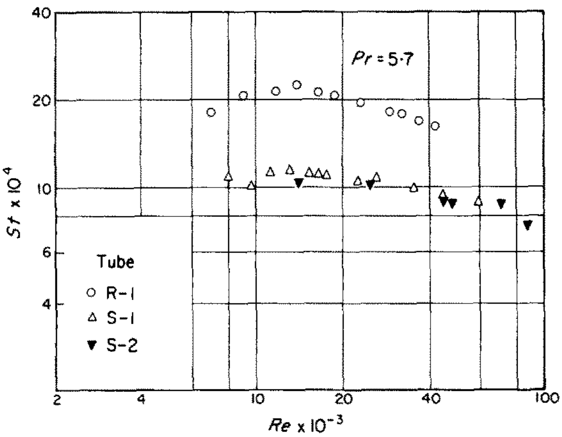

FIG. 4. Stanton number as a function of Reynolds number in test sections S-1, S-2 and R-1 with water.

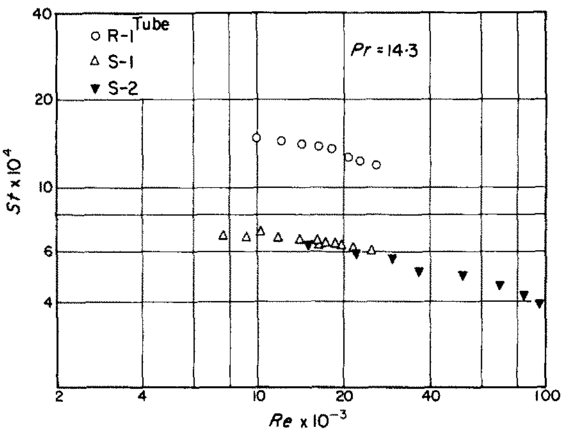

FIG. 5. Stanton number as a function of Reynolds number in test sections S-1, S-2 and R-1 with aqueous ethylene glycol.

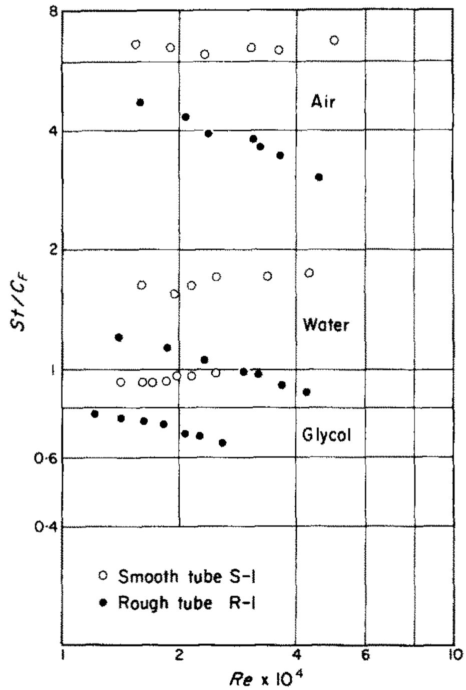

FIG. 6. Stanton number–friction factor ratio for test sections S-1 and R-1 at various Prandtl numbers.

shows that St/C_F for the rough surface increases as the Reynolds number decreases. An earlier study by the authors [8] has shown this trend and also the fact that rough pipes become more efficient than smooth ones in the transition region for high Prandtl number fluids. A recent study by Townes and Sabersky [9] on rough surface momentum transfer provides an insight into this type of behaviour. In the roughness transition region flow within the roughness troughs is unsteady and a strong secondary flow takes place.

Radial temperature profiles for the rough surface test section are presented in Figs. 7–9 for each of the fluids that was studied. It is obvious from these figures that if the temperature is expressed non-dimensionally as t^+ it exhibits a semi-logarithmic relationship with y/R for the region away from the immediate vicinity of the wall. The results are, therefore, similar to the smooth tube temperature and velocity profiles expressed as t^+ and u^+ respectively. While there is similarity there is a distinct

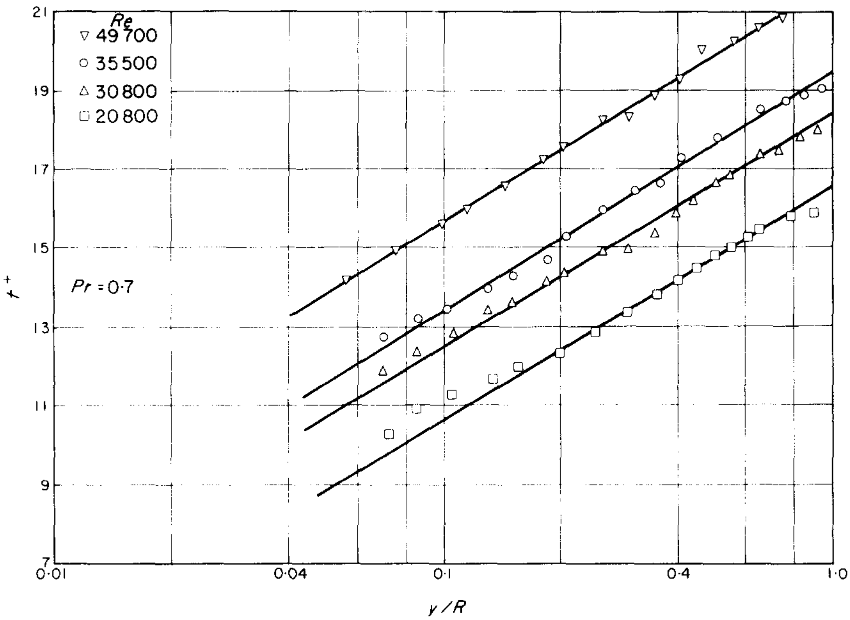

FIG. 7. Radial temperature profiles in air for test section R-1.

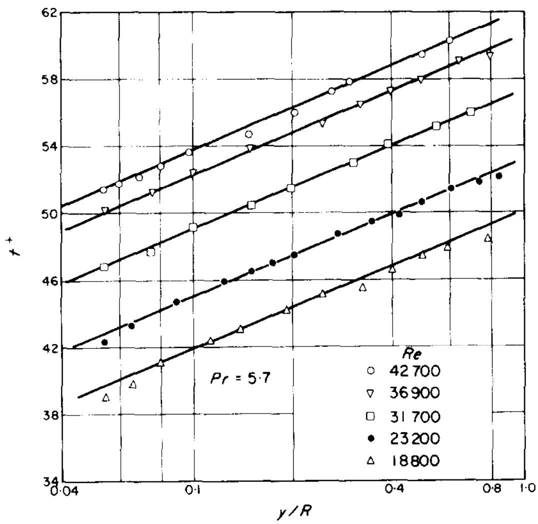

FIG. 8. Radial temperature profiles in water for test section R-1.

difference between the logarithmic slopes of rough surface temperature profiles and those of the velocity profiles of Nikuradse. In momentum transfer, the logarithmic slope of the velocity profile remains constant at 2·5 regardless of whether the surface is rough or smooth, i.e.

$$\frac{\mathrm{d}u^+}{\mathrm{d}y^+} = \frac{2\cdot 5}{y^+} \text{ (rough or smooth).} \tag{6}$$

In heat transfer the temperature gradient can be represented by,

$$\frac{\mathrm{d}t^+}{\mathrm{d}y^+} = \frac{A_R}{y^+} \tag{7}$$

but the constant A_R changes when the wall is roughened. Therefore, unlike the smooth and rough velocity profiles, the rough tube temperature profile cannot be expressed in terms of a simple shift in the smooth tube profile. The constant A_R depends on the Prandtl number and the roughness. Table 2 shows a comparison of the logarithmic slopes of the temperature profiles for smooth and rough surfaces. Values of A for the smooth tube have been taken from [1].

The differences in slope of the dimensionless temperature profiles between smooth and rough surfaces suggest that the mechanism of turbulent heat transfer is different in the turbulent core. An estimate of the magnitude of the effect of

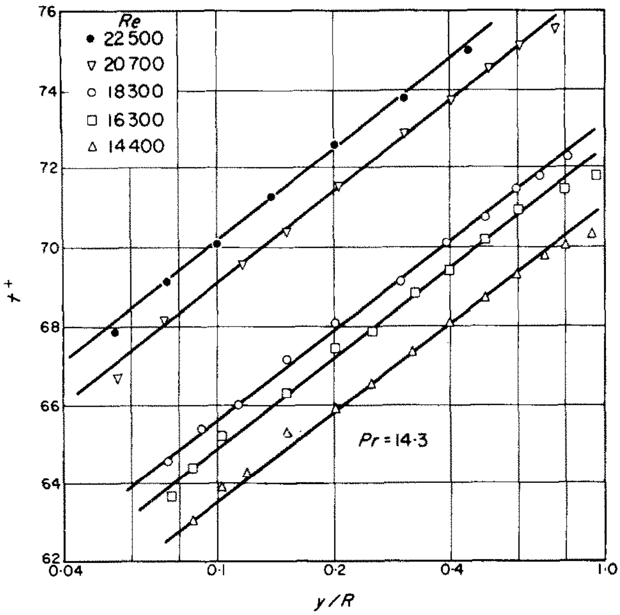

FIG. 9. Radial temperature profiles in aqueous ethylene glycol for test section R-1.

Table 2

Pr	Rugh surface A_R	Smooth surface A
0·7	2·7	2·2
5·7	3·5	2·6
14·3	3·4	2·6

wall roughness at constant Reynolds number may be made by calculating the eddy diffusivity defined as follows for a constant flux wall:

$$\dot{q}/\dot{q}_w = \left(\frac{1}{Pr} + \frac{\epsilon_H}{v}\right)\frac{dt^+}{dy^+}. \tag{8}$$

The axial temperature gradient may be assumed to be independent of radial position for constant $\dot{q}_w$ and hence the dimensionless heat flux ratio $\dot{q}/\dot{q}_w$ may be calculated from:

$$\dot{q}/\dot{q}_w = \frac{2R}{r}\int\limits_0^{r/R}\left(\frac{u}{U_B}\right)\left(\frac{r}{R}\right)d\left(\frac{r}{R}\right)$$

$$= 2R\int\limits_0^{\mathscr{R}}\left(\frac{u}{U_B}\right)\mathscr{R}\,d\mathscr{R}. \tag{9}$$

The results of the calculation using equation (2) for the velocity distribution across the tube, $C_F = 0{\cdot}0185$, are shown in Fig. 10. Also shown are the heat flux ratios for turbulent flow in a smooth tube ($Re = 30000$) and for laminar flow. At $y/R = 0{\cdot}5$, the radial heat flux ratio is about 10 per cent greater in rough than in smooth tubes.

The dimensionless gradient $dt^+/dy^+ = A_R/y^+$ may be obtained from the experimental curves of t^+ against log y/R, and ϵ_H/v may be calculated from equation (8). The results of the calculation are shown in Fig. 11 for air as plots of ϵ_H/v and ϵ_M/v against y/R for the smooth and rough pipes at a Reynolds number of 40000. The eddy diffusivity of heat is seen to be about 50 per cent higher in the rough tube than the smooth one. If the comparison is made at the same wall shear stress (equal y^+), the eddy diffusivity of heat is somewhat less in rough pipes than smooth ones because of the difference in dimensionless temperature gradients.

The results are also plotted in Fig. 12 as turbulent Prandtl number $Pr_t(\epsilon_M/\epsilon_H)$ against radial position for air and aqueous ethylene

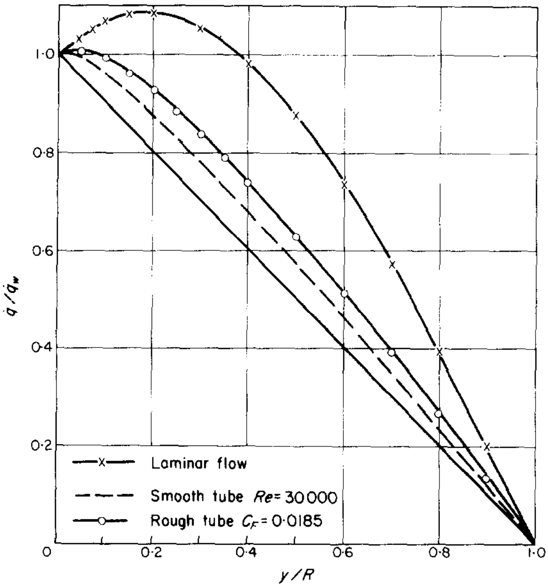

FIG. 10. Radial heat flux distribution for smooth and rough pipes.

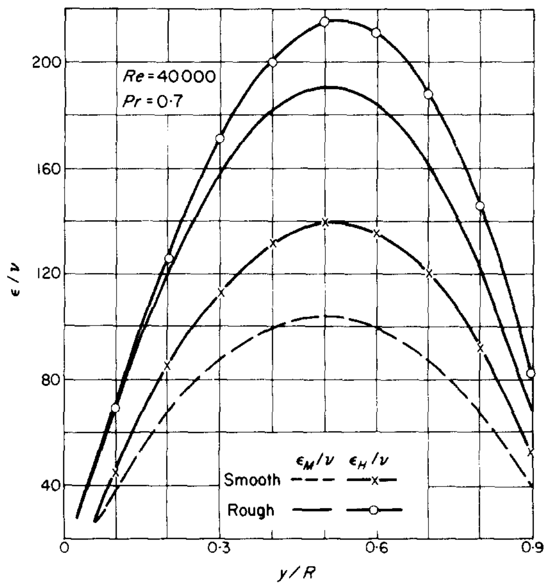

FIG. 11. Radial distribution of thermal and momentum diffusivities for smooth and rough pipes.

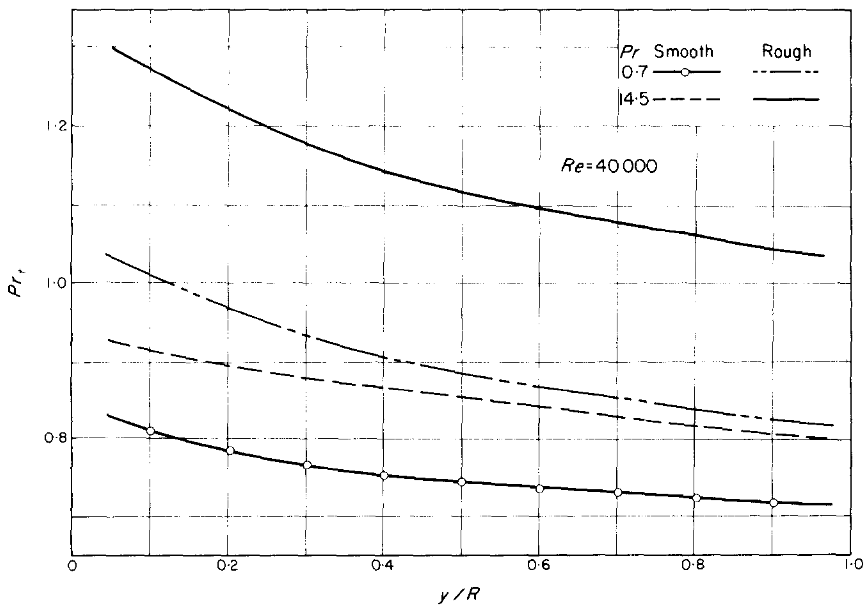

FIG. 12. Turbulent Prandtl number Pr_t against radial position y/R for air and aqueous ethylene glycol.

glycol. The curves show that roughness and Prandtl number have an effect on the turbulent transfer mechanism. The effect of Prandtl number in smooth pipes is discussed in [1]. The slight increase in dimensionless slope A with Pr suggests that molecular diffusion of heat from eddies is a significant mechanism in turbulent heat transfer in both rough and smooth tubes.

The roughness has an even more pronounced effect on the resistance to heat transfer near the wall. This is shown by the dimensionless temperature $(t_w - t)/(t_w - t_B)$, which is about 30 per cent greater in rough than in smooth pipes at any radial position in the turbulent core. This means that the *relative* resistance to heat transfer is greater in the turbulent core of rough pipes than in the turbulent core of smooth pipes, in spite of the larger eddy diffusivity there.

The general increase in t^+ at a given y^+ or y/R with increasing Prandtl number has also been observed in smooth pipes [1], and is consistent with a shift in relative resistance from the turbulent core to the wall region. The increase in t^+ with increasing Reynolds number observed in the rough pipe is *not* observed in smooth pipes. This result suggests that stagnant areas around roughness elements become relatively more important to the overall resistance to heat transfer as the Reynolds number is increased.

Development of a universal temperature profile law for rough pipes

Figures 7–9 show that radial temperature profiles for turbulent flow in a rough pipe can be represented by:

$$t^+ = A_R \ln y/R + \psi. \tag{10}$$

The function ψ is undefined but should depend on the parameters Re^*, C_F and Pr.

The experimentally determined values of the intercept value are tabulated in Table 3 for the three fluids evaluated at the appropriate Reynolds number.

Nikuradse has shown that dimensionless velocities in rough pipes are given by:

$$u^+ = 2{\cdot}5 \ln y/R + 3{\cdot}75 + \sqrt{(2/C_F)} \tag{11}$$

By analogy, one might expect dimensionless temperature profiles to be given by an equation of the form:

$$t^+ = A_R \ln y/R + f(Re^*, Pr, C_F). \tag{12}$$

in which

$$f(Re^*, Pr, C_F) = \left[f_1(Re^*) + \sqrt{\left(\frac{2}{C_F}\right)}\right] f_2(Pr).$$

Empirical correlation of the experimental values of ψ, Re^* and Pr, assuming simple relations, gives:

$$t^+ = A_R \ln y/R + [0{\cdot}155\, Re^{*\,0{\cdot}54} + \sqrt{(2/C_F)}]\, Pr^{0{\cdot}5}. \tag{13}$$

The calculated and experimental values of ψ tabulated in Table 3 show reasonable agreement. The general effect of roughness on the slope A_R and the validity of equation (13) for other roughness patterns remains to be determined.

Table 3. Measured ψ and ψ calculated from equation (13), $t_b \simeq 75°F$

$Pr \simeq 0{\cdot}7$ (Air)				$Pr \simeq 5{\cdot}7$ (Water)				$Pr \simeq 14{\cdot}3$ (Glycol solution)			
Re	$t_w - t_b$	$\psi_{meas.}$	$\psi_{calc.}$	Re	$t_w - t_b$	$\psi_{meas.}$	$\psi_{calc.}$	Re	$t_w - t_b$	$\psi_{meas.}$	$\psi_{calc.}$
20800	35·2	16·6	16·6	18800	11·6°F	50·0	46·0	14400	10·93°F	71·0	68·6
30800	28·6	18·4	18·4	23200	9·96	53·3	49·0	16300	9·77	72·5	72·0
35500	35·3	19·4	19·2	31700	7·96	57·4	54·4	18300	8·89	73·3	74·5
49700	29·01	22·2	21·3	36900	7·14	60·7	56·9	20700	8·36	76·8	76·5
				42700	6·33	62·2	60·0	22500	7·83	77·7	78·1

2. HEAT-TRANSFER COEFFICIENTS IN ROUGH PIPES OF KNOWN SURFACE GEOMETRY

Introduction

Very few, if any adequate laws have been developed for predicting the experimentally determined increase in heat-transfer coefficients resulting from artificial surface roughness. The absence of such laws for the design of artificially roughened heat-transfer surfaces which have been proposed and used in gas-cooled nuclear reactors and other heat exchange equipment is due in large part to a shortage of reliable heat-transfer data for more than a few geometric patterns.

This part of the paper describes the results of heat-transfer measurements to seven surfaces of exactly known geometry. Air ($Pr = 0{\cdot}7$), water ($Pr = 5{\cdot}7$) and ethylene glycol ($Pr = 15{\cdot}5$) were used as the test fluids and the flow covered a range of Reynolds numbers from 10000 to 100000.

A model based on the temperature profiles of Section 1 is based on an assumed analogy between heat transfer and momentum transfer in rough pipes.

Such a model is not entirely appropriate since the temperature profiles plotted as t^+ against $\ln y/R$ show a Reynolds number dependence as well as the expected Prandtl number dependence. However, the profiles follow similar algebraic expressions, which suggests that an assumption of similarity may not be without merit.

Previous work

Most rough surface heat-transfer studies in the past have used air as the test fluid not only because of its practical importance, but also because its Prandtl number is near unity. Studies in aerodynamics [11] have shown the effect of roughness on boundary-layer transition and on aerodynamic heating. Heat-transfer studies by Burgoyne, Burnett and Wilkie [12], Kemeny and Cyphers [13], Sheriff and Gumley [14], and Walker and Rapier [15] in conjunction with the United Kingdom Atomic Energy Commission have provided data for heat-transfer coefficients in turbulent flow in rough annuli with air. In 1956, Nunner [16] proposed the following equation for rough surface heat transfer as a result of an extensive study with air,

$$St = \frac{C_F/2}{1 + 1{\cdot}5\, Re^{-\frac{1}{8}}\, Pr^{-\frac{1}{6}}\,(Pr\, C_F/C_{FS} - 1)} \qquad (15)$$

where C_F/C_{FS} = the ratio of rough to smooth friction factors at the same Reynolds number. In deriving equation (15), Nunner postulated that the viscous wall layer behaves almost exactly the same in a rough tube as in a smooth tube at the same Reynolds number, and therefore only the resistance of the turbulent core is affected by roughness. Another consequence of this model is the effect of roughness on the heat-transfer coefficient, which should increase as the Prandtl number decreases. This contradicts later experimental studies [17–19]. In 1961, Dipprey and Sabersky [19] proposed a heat-transfer similarity law based on heat transfer to water as follows:

$$St = \frac{C_F/2}{1 + [\sqrt{(C_F/2)}]\,(\gamma e^{*\,0{\cdot}2}\, Pr^{0{\cdot}44} - 8{\cdot}48)} \qquad (16)$$

where

$$e^* = \frac{e_s}{D} Re \sqrt{(C_F/2)}.$$

Arguments in support of this law are well presented but the law does not take into account the important difference between velocity and temperature profiles in rough pipes discussed previously. The heat-transfer similarity law provides strong evidence that the friction velocity is a more suitable parameter than the flow velocity for predicting rough surface heat transfer. Several other studies [18, 20] have also developed correlations using u^* as the main parameter. However, correlations based only on the heat-transfer coefficient cannot adequately and generally predict heat-transfer rates from rough surfaces because such correlations ignore the effect of roughness on the detailed structure of the resistances to heat transfer. These details are revealed at least in part by temperature profiles as discussed in Section 1.

Experimental

Two dimensional roughnesses in pipes are usually made by machining the inside of a smooth tube, whereas the effect of natural roughness is usually tested by using large commercial pipes. In each case the roughness height is difficult to measure and the surface, particularly in small diameter pipes cannot be seen without cutting the pipe in half. The method of making rough pipes described here affords test sections of exactly known roughness patterns and with easily and accurately measurable characteristics.

The desired roughness was first imprinted on a 2 × 20-in sheet of brass shimstock 0·003-in thick with a special roughness pattern and a roller. A sheet of hard rubber 0·25 × 3 × 21 in served as a backing and provided the compressibility needed to imprint the pattern. As a result, any roughness pattern may be obtained, the surfaces are readily visible and the indivudual roughness protrusions are the same height and hence they can easily be measured with a micrometer. The brass sheet was cut to its final size 1·625 × 18 in, after the roughness pattern had been imprinted on it. The actual rough pipe was made by carefully wrapping the brass sheet around a glass tube, hard soldering the seam and keeping the resulting cylinders circular in cross-section throughout its entire length. When the cylinder had been soldered it was tested for leaks and repaired where necessary. Eight 32 gauge copper–constantan thermocouples were attached directly to the outside wall of the brass cylinder at distances of 4, 5·5, 7, 8·5, 10, 11·5, 13 and 14 in from one end. All the thermocouple leads were wired to the cylinder to minimize disturbances in heat-transfer distribution. The cylinder was then placed inside a shell which formed the outside of the heat-transfer test section. This shell was made from a standard 1-in dia. copper tube 14-in long. After the bottom of the shell was packed with asbestos powder, the shell was heated to approximately 400°F and molten solder (50% lead–50% tin) was poured into the annulus formed between the shell and the brass cylinder. When the pipe had cooled to room temperature the glass tube inside the brass cylinder was removed.

The outer surface of the test section was wrapped with a Teflon film 0·004-in thick in order to insulate it from the electric heating element. The heating element was made from a nichrome resistance ribbon (0·03125 × 0·005 in) 0·692 Ω/ft, which was wrapped uniformly around the Teflon film. To prevent heat losses the test section was insulated with 0·5 in layer of glass wool. The completed test sections are shown in Fig. 13.

Smooth tube S-2 was made in a fashion similar to that described above except that the thin brass cylinder was replaced with a standard 0·625-in copper tube, 18 in. in length. The roughness patterns made are listed below:

Test sections R-6, R-7, and R-8 were made with

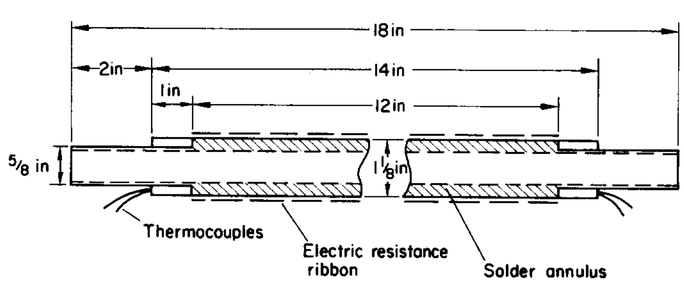

FIG. 13. Half-inch diameter test section.

Roughness patterns

Tube	Description
S-2	smooth tube
R-1	rough pipe, square wire mesh described in Section 1
R-2	square array roughness pattern made by soldering 20–25 mess copper balls 0·125 in apart on a backing plate
R-3	triangular array roughness pattern made by soldering 20–25 mesh copper balls 0·125 in apart on a backing plate
R-4	random roughness pattern made by gluing 14–16 mesh carborundum particles on a backing plate
R-5	screen roughness made by soldering a regular 12 mesh brass screen on a backing plate
R-6	inverted pattern to tube R-5
R-7	inverted pattern to tube R-3
R-8	inverted pattern to tube R-2

the same roughness patterns as in test sections R-5, R-3, and R-2 respectively, but with the surface inverted, so that hills become valleys.

Water and 30% aqueous ethylene glycol solution were circulated through the test sections with a 5 hp centrifugal pump. A cold water shell and tube heat exchanger controlled the temperature of the test fluids. When air was used as the test fluid, the fluid section was disconnected and air was provided by a blower.

Heat input and friction factors were determined as described in Section 1 of this paper.

Results

Friction factors are presented as log C_F vs. log Re for all the rough pipes used in the present study in Figs. 14 and 15. These figures show that the fully rough regime is reached for all pipes once the Reynolds number has exceeded 10000. The equivalent sand roughness was calculated using equation (3), and e_s/D for each pipe is given in Table 4.

Heat-transfer coefficients. Typical heat-transfer coefficients for the rough pipes are plotted in Figs. 16–18 as Stanton number against Reynolds number on logarithmic coordinates with the Prandtl number as a parameter.† Unlike the friction factor, the Stanton number shows a strong Reynolds number dependence in the fully rough regime.

Table 5 shows a list of the fully rough friction factors in descending order for all the rough pipes used in the present study. The same table also lists the Stanton numbers at $Re = 30000$ for each Prandtl number studied. The relative magnitude of the Stanton number appears to be nearly the same as that of the friction factors. Variations in the order are undoubtedly due to the different types of roughness studied. These differences are not accounted for by any correlation of rough pipe heat transfer, including the present one, and show the need for further experimental study of the detailed heat-transfer process.

Table 4. Comparison of the equivalent sand roughness with the actual measured roughness height

Tube	C_F (fully rough)	Measured e/D	Equivalent sand roughness e_s/D
R-2	0·0134	0·021	0·028
R-3	0·0165	0·025	0·040
R-4	0·0124	0·018	0·026
R-5	0·0255	0·026	0·095
R-6	0·0230	0·026	0·074
R-7	0·0126	0·022	0·021
R-8	0·0157	0·024	0·036

Prediction of heat-transfer rates from a rough surface. Fully developed turbulent temperature profiles in rough pipes with constant heat flux can be expressed by equation (13) for the pipe studied. Equation (13) may be applied to other rough pipes if it is assumed that C_F (or e_s/D) characterizes the roughness for heat transfer. This assumption is certainly untrue, in general, but agrees with the trend shown in Table 5.

† Complete numerical data are available from the Documentation Centre for Unpublished Data, National Research Council, Ottawa 2, Canada.

Table 5. Fully rough friction factors and Stanton numbers for all rough pipes at a Reynolds number of 30000

Tube	Friction factor C_F	Stanton number St $Pr = 0{\cdot}7$	$Pr = 6{\cdot}0$	$Pr = 14{\cdot}3$
R-5	0·0255	0·0090	0·00205	0·0010
R-6	0·023	0·0065	0·00185	0·0011
R-1	0·0185	0·0069	0·00185	0·00116
R-3	0·0165	0·0068	0·00160	0·00105
R-8	0·0157	0·0070	0·00190	0·00105
R-2	0·0134	0·0063	0·00150	0·00088
R-7	0·0126	0·0060	0·00150	0·00086
R-4	0·0124	0·0060	0·00140	0·00072
S-2	0·0056	0·0037	0·00105	0·00058

The mean velocity u_B and mean temperature t_B may be expressed in dimensionless form by:

$$t_B^+ = A_R \ln y_B/R + \psi \qquad (15)$$

$$u_B^+ = 2{\cdot}5 \ln y_B/R + \varepsilon \qquad (16)$$

where y_B is the radial position at which $t^+ = t_B^+$ and $u^+ = u_B^+$, respectively.

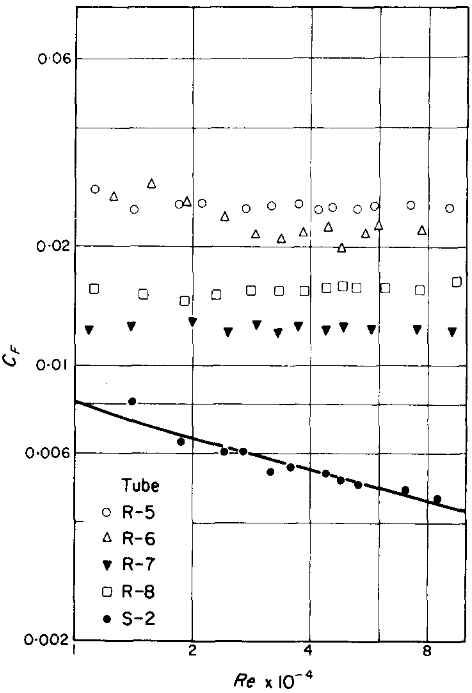

FIG. 15. Friction factor curves for test sections S-2, R-5, R-6, R-7 and R-8.

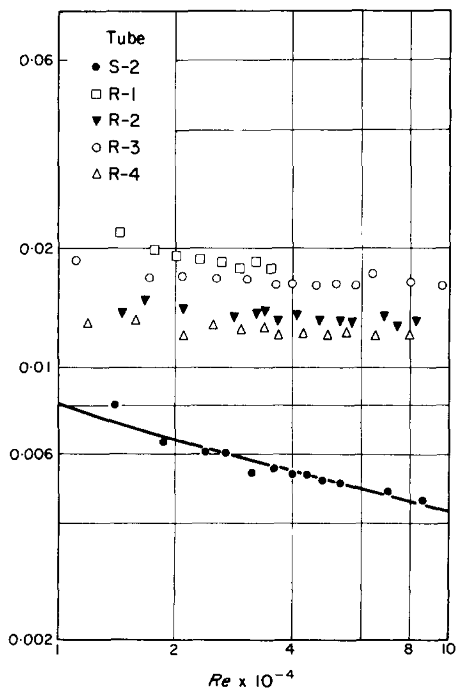

FIG. 14. Friction factor curves for test sections S-2, R-2, R-3 and R-4.

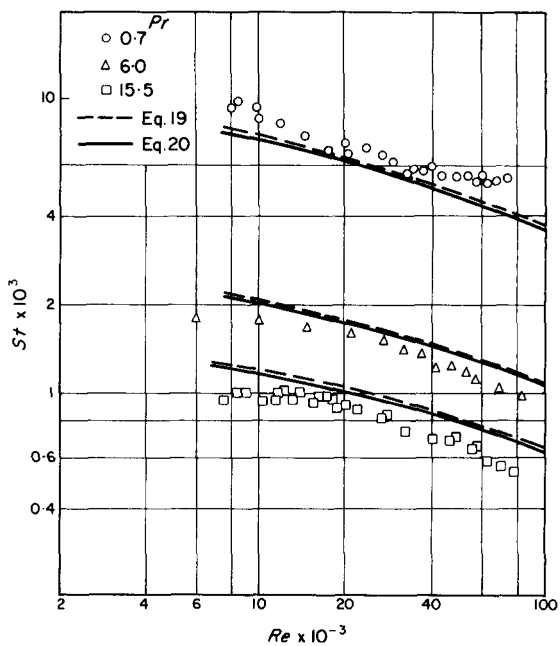

FIG. 16. Stanton number as a function of Reynolds number for test section R-2.

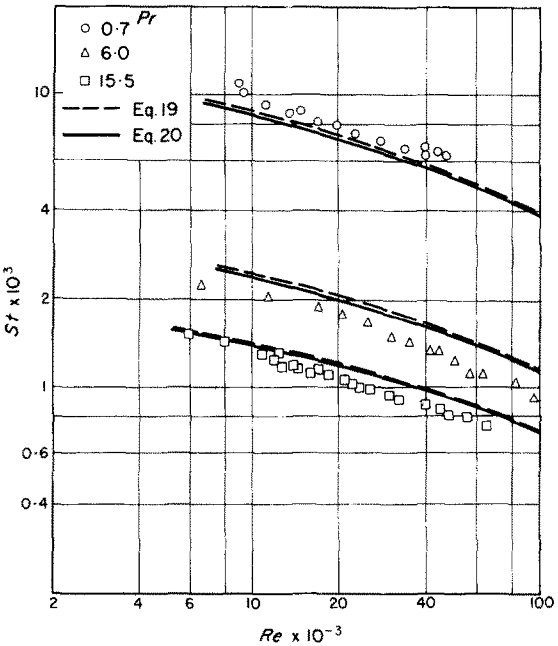

FIG. 17. Stanton number as a function of Reynolds number for test section R-3.

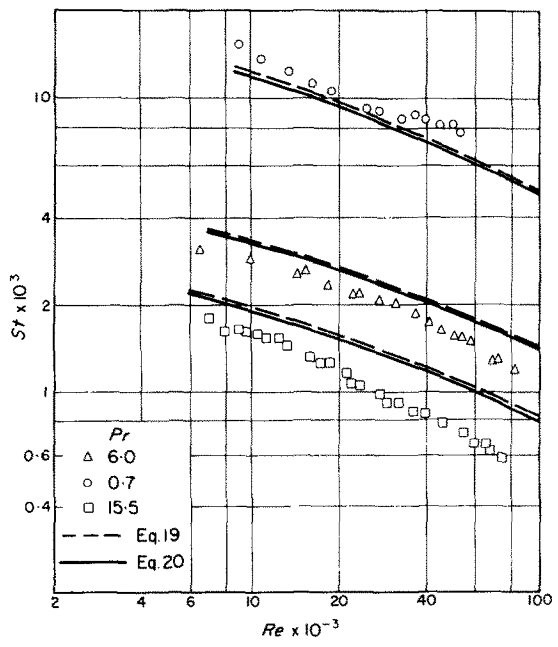

FIG. 18. Stanton number as a function of Reynolds number for test section R-5.

In general y_B in equation (15) is not the same as y_B in equation (16) but if they are assumed the same, equation (16) may be subtracted from equation (15) to give:

$$t_B^+ - u_B^+ = \psi - \varepsilon + \frac{A_R - 2{\cdot}5}{2{\cdot}5}(u_B^+ - \varepsilon). \quad (17)$$

Since

$$u_B^+ = \sqrt{(2/C_F)}$$

$$t_B^+ = \frac{\sqrt{(C_F/2)}}{St}.$$

Equation (17) may be rearranged to give:

$$St = \frac{\sqrt{C_F/2}}{\psi - 3{\cdot}75\, A_R/2{\cdot}5}. \quad (18)$$

The constant A_R varies from 2·7 to 3·5 over a Prandtl number range of 0·7–14·3 for one particular type of roughness as shown in Table 2. It may be tentatively assumed equal to 3·0 pending further experimental work to determine its exact dependence on roughness pattern and *Pr*. Heat-transfer coefficients can then be predicted from the relatively simple expression:

$$St = \frac{\sqrt{(C_F/2)}}{\psi + 4{\cdot}5}. \quad (19)$$

A more rigorous derivation in which y_B is assumed to be the same for t_B and u_B results in:

$$\frac{1}{St} = \int_{y/R=0}^{y/R=a} u^+ t^+ \mathscr{R}\, d\mathscr{R} + \int_{y/R=a}^{y/R=1} u^+ t^+ \mathscr{R}\, d\mathscr{R} \quad (20)$$

where "a" is the distance from the wall at which the turbulent core begins, and is generally assumed to be given by:

$$a = \frac{1}{15}\frac{e_s}{D}. \quad (21)$$

Together with all the experimental Stanton numbers, the Stanton numbers predicted from equation (19) are shown as dotted lines and from equation (20) as solid lines on Figs. 16–18. The very slight difference between the predictions of equations (19) and (20) does not justify the use of the more rigorous equation over the range of experiments. More than 67 per cent of the predicted Stanton numbers deviate less than 25 per cent from the measured values.

A comparison of the equations used for the prediction of rough surface heat transfer developed by Nunner, Dipprey and in the present study are shown in Figs. 19–21. For low Prandtl number fluids like air (Fig. 19), there is little difference between the equations. However, as the Prandtl number increases the difference between the equations also increases. For all Prandtl numbers, values predicted by Nunner's equation, which was based on measurements in air, are too low.

Each equation contains empirical constants

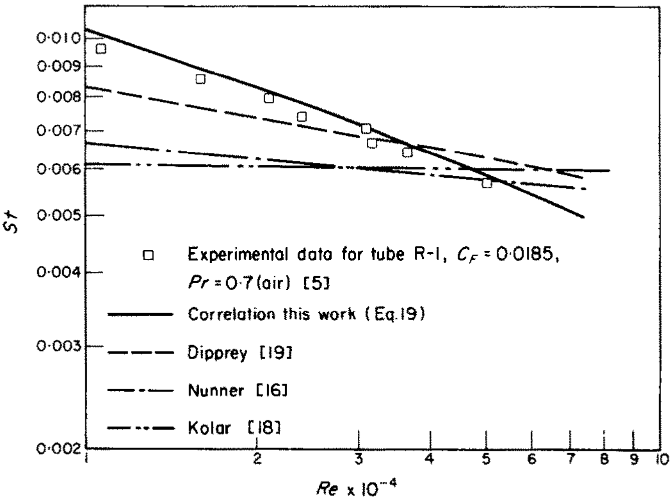

FIG. 19. Comparison of proposed correlations for heat transfer with data for air—*St* against *Re*.

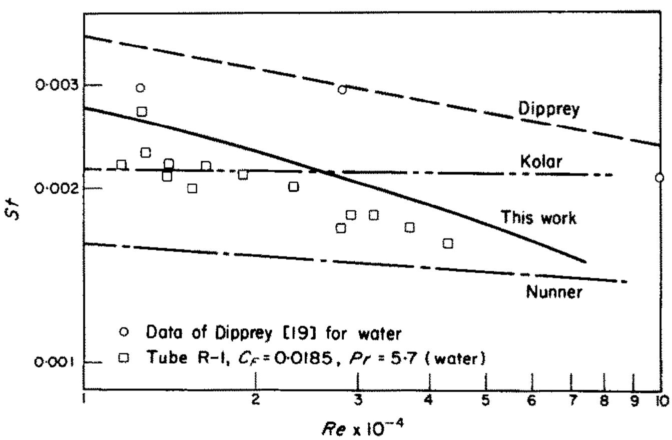

FIG. 20. Comparison of proposed correlations for heat transfer with data for water—*St* against *Re*.

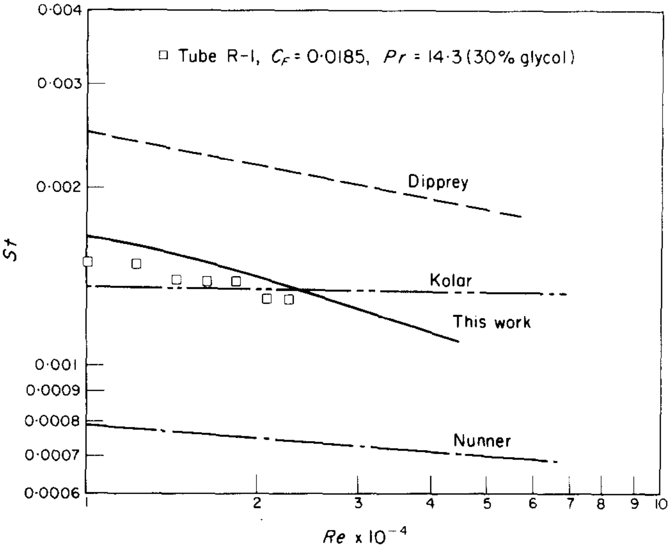

FIG. 21. Comparison of proposed correlations for heat transfer with data for 30% ethylene glycol—*St* against *Re*.

determined from the experimental data of each study. Not surprisingly, the equations give good fits only for the data from which they were derived. For instance, Dipprey's experimental points and predicted values appear to be higher than most other workers have obtained [18, 20]. Small local variations in the wall thickness of Dipprey's pipes could lead to errors in the calculation of the inside wall temperature, particularly at high wall heat fluxes. Moreover, a small error in the estimated wall thickness could lead to a relatively large systematic error in the calculated wall temperature. This and other studies have shown that empirical correlations involving only the heat-transfer coefficient are not adequate.

The model presented in equation (19) predicts heat-transfer coefficients of the present work with a standard deviation of ± 25 per cent. The best of the other semi-empirical correlations appears to be that of Kolar which predicts the present data with about the same reliability.

The mediocre reliability of equation (19) in predicting the heat-transfer results undoubtedly results from the assumption implicit in it that C_F and hence e_s/D completely characterizes the effect of roughness on temperature profiles.

REFERENCES

1. R. A. GOWEN and J. W. SMITH, The effect of the Prandtl number on temperature profiles for heat transfer in turbulent pipe flow, *Chem. Engng Sci.* **22**(12), 1701–1711 (1967).
2. J. NIKURADSE, Laws of flow in rough pipes, *Forsch.-Hft. Ver. Dt. Ing.* 361 Series B4 (1933); translation N.A.C.A., T.M. 1292 (1950).
3. W. L. MOORE, An experimental investigation of boundary-layer development along a rough surface, State University of Iowa, Ph.D. dissertation (August 1951).
4. F. H. CLAUSER, The turbulent boundary layer, *Adv. Appl. Mech.* **4**, 1–51 (1956).
5. R. A. GOWEN, A study of forced convection heat transfer from smooth and rough surfaces, Ph.D. thesis, University of Toronto, Department of Chemical Engineering (1967).
6. E. LOGAN and J. B. JONES, Flow in a pipe following an abrupt increase in surface roughness, *J. Bas. Engng* **85**(1), 35 (1963).
7. C. A. SLEICHER and M. TRIBUS, *Recent Advances in Heat and Mass Transfer*. McGraw-Hill, New York (1961).
8. R. A. GOWEN and J. W. SMITH, Heat transfer efficiency in rough pipes at high Prandtl number, *A.I.Ch.E. Jl* **11**, 941–942 (1965).
9. H. W. TOWNES and R. SABERSKY, Experiments in flow over a rough surface, *Int. J. Heat Mass Transfer* **9**, 729–738 (1966).

10. J. W. SMITH, R. A. GOWEN and B. WASMUND, Eddy diffusivities and temperature profiles for turbulent heat transfer to water in pipes, *A.I.Ch.E. Symp. Ser.* 77 **63**, 92–101 (1967).
11. M. G. DUNN, Effect of three dimensional roughness elements on boundary layer and aerodynamic heating, *J. Spacecraft Rockets* **1**, 68 (1964).
12. T. B. BURGOYNE, P. BURNETT and D. WILKIE, Forced convection heat transfer from surfaces roughened by transverse ribs, U.K.A.E.A. TRG Report 781 (W) (1964).
13. C. A. KEMENY and J. A. CYPHERS, Heat transfer and pressure drop in an annular gap with surface spoilers, *J. Heat Transfer* **83**(2), 189 (1961).
14. N. SHERIFF and P. GUMLEY, Heat transfer and friction properties of surfaces with discrete roughnesses, U.K.A.E.A. TRG Report 929 (1965).
15. V. WALKER and A. C. RAPIER, Fuel element heat transfer, *J. Br. Nucl. Energy Soc.* **2**(2), 268–275 (1963).
16. W NUNNER, Heat transfer and pressure drop in rough pipes, *ForschHft. Ver. Dt. Ing.* 361 Series B4 (1933); Translation A.E.R.E. lib/trans 786 (1958).
17. V. GOMELAURI, Influence of two-dimensional artificial roughness on convective heat transfer, *Int. J. Heat Mass Transfer* 7, 653 (1964).
18. V. KOLAR, Heat transfer in smooth and rough tubes,
19. D. F. DIPPREY and R. SABERSKY, Heat and momentum transfer in smooth and rough tubes at various Prandtl numbers, *Int. J. Heat Mass Transfer* **6**, 329–353 (1963).
20. P. R. OWEN and W. R. THOMSON, Heat transfer across rough surfaces, *J. Fluid Mech.* **15**, part 3, 321–334 (1963).

Résumé—Les profils radiaux de température ont été obtenus dans un tube rugueux de 50,8 mm de diamètre intérieur dont la rugosité équivalente de sable était égale à 0,05 pour des nombres de Prandtl de 0,7, 5,9 et 14,3 dans une gamme de nombres de Reynolds de 10000 à 50000. Les diagrammes de t^+ sont linéaires en fonction de Log y/R comme dans le cas de u^+ pour des tubes rugueux et lisses, mais la pente dépend du nombre de Prandtl et, par déduction, de la rugosité. La valeur de t^+ à l'intersection avec la droite d'équation : Log $y/R = 0$, dépend fortement du nombre de Reynolds, à la différence de u^+ dans l'écoulement turbulent dans un tube rugueux. On présente une expression pour la relation entre t^+ et log y/R, mais la dépendance de la pente A_R en fonction de la rugosité reste à déterminer. L'efficacité du transport de chaleur St/C_F était moindre dans les tubes rugueux que dans les tubes lisses pour tous les fluides étudiés, mais la différence relative devient plus faible à des nombres de Prandtl élevés et dans la région de transition vers la turbulence. Les coefficients de frottement et de transport de chaleur ont également été mesurés dans sept tubes regueux différents de diamètre intérieur égal à 12,7 mm et dont la surface a une géométrie connue. Les rugosités équivalentes de sable variaient de 0,021 à 0,095 pour les tuaux étudiés. Une équation semiethéorique basée sur les profils de températures obtenus dans le tuyau de 50,8 mm prédit convenablement les résultats de l'étude actuelle et ceux de Nunnter pour l'air. Elle sous-estime les résultats de Dipprey pour l'eau.

Zusammenfassung—Radiale Temperaturprofile wurden in einem Rohr von 50 mm Innendurchmesser erhalten bei äquivalenten Sandrauhigkeiten von 0,05, Prandtl-Zahlen von 0,7, 5,9 und 14,3 in einem Reynolds–Zahlenbereich von 10000–50000. Diagramme von t^+ über log y/R sind linear wie im Falle von u^+ für rauhe und glatte Rohre, aber die Neigung hängt von der Prandtl–Zahl ab und -so wird gefolgert- auch von der Rauhigkeit. Der t^+-Abschnitt bei log $y/R = 0$ hängt stark von der Reynolds–Zahl ab, ungleich u^+ in turbulenter rauher Rohrströmung. Eine Beziehung zwischen t^+ und log y/R wird angegeben, aber die Abhängigkeit der Neigung A_R von der Rauhigkeit bleibt noch zu bestimmen. Der Wärmeübergangs-wirkungsgrad St/C_F war in rauhen Rohren kleiner als in glatten für alle untersuchten Flüssigkeiten, aber die gegenseitigen Unterschiede wurden kleiner bei höheren Prandtl–Zahlen und im turbulenten Übergangs-gebiet. Reibungskoeffizienten und Wärmeübergangskoeffizienten wurden gemessen für sieben verschiedene rauhe Rohre von 12 mm Innendurchmesser und bekannter Oberflächengeometrie. Die äquivalenten Sandrauhigkeiten erstreckten sich von 0,021 bis 0,095. Eine halbtheoretische Gleichung, die auf den Temperaturprofilen beruht, die im 50 mm Rohr erhalten wurden, gibt die gegenwärtigen Ergebnisse und die Ergebnisse von Nunner für Luft zufriedenstellend wieder. Sie liefert zu kleine Werte für die Ergebnisse von Dipprey für Wasser.

Аннотация—Получены распределения температуры по радиусу трубы с внутренним диаметром $\phi 2''$, эквивалент песочной шероховатости которой составляет 0,05 для чисел Прандтля 0,7, 5,9 и 14,3 в диапазоне чисел Рейнольдса от 10000 до 50000. Зависимости t^+ и u^+ от $\log y/R$ являются линейными для шероховатых и гладких труб, а угол наклона определяется числом Прандтля и шероховатостью. В отличие от u^+ значение t^+ при $\log y/R = 0$ сильно зависит от Re в шероховатой трубе при турбулентном течении. Приводится зависимость t^+ от $\log y/R$ и подлежит определению зависимость угла наклона A_R от шероховатости. Эффективность теплообмена St/C_F меньше в шероховатых трубах, чем в гладких для всех исследуемых жидкостей. Относительная разность становится меньше при большем числе Прандтля и в области перехода от ламинарного течения в турбулентное. Также измерены коэффициенты трения и теплообмена для семи различных труб $\phi 2''$ с известной геометрией поверхности. Эквивалентные песочные шероховатости изменялись от 0,021 до 0,095 в исследуемых трубах. Результаты данного исследования и результаты Нуннера для воздуха получены с помощью полуэмпирического соотношения, основанного на распределениях температуры в трубе $\phi 2''$. Результаты Диппри для воды не коррелируются полуэмпирическим уравнением.